

1 **Analysis of Spatio-temporal rainfall trends across southern African biomes between 1981**
2 **and 2016**

3
4 Farai Maxwell Marumbwa^{a*}, Moses Azong Cho^{b,c} and Paxie Chirwa^d

5 ^aCentre for Environmental studies, University of Pretoria, Pretoria 0002, South Africa

6 ^bNatural Resources and Environment Unit, The Council for Scientific and Industrial Research (CSIR), P.O. Box
7 395, Pretoria 0001, South Africa

8 ^cDepartment of Plant and Soil Science, University of Pretoria, Pretoria 0002, South Africa

9 ^dForest Science Postgraduate Programme, Department of Plant and Soil Sciences, University of Pretoria, Pretoria,
10 South Africa

11
12 * Corresponding Author email: maxmarumbwa@gmail.com

13
14 **Abstract**

15
16 Southern African biomes experience significant changes in the distribution of rainfall that are
17 linked to El Niño–Southern Oscillation. As such, an understanding of the spatio-temporal
18 rainfall trends is key in predicting rainfall patterns as well as validation of climate change
19 projections. Currently, the available information on rainfall trends in southern Africa is scanty
20 with most studies focusing either on the spatial or the temporal dimension at localised levels.
21 The novelty of this study is its regional aspect (i.e. all of southern African arid and semi-arid
22 biomes) and the simultaneous integration of space and time in rainfall trend analysis through
23 the use of space time rainfall cube. In this study, we simultaneously examined spatial and
24 temporal rainfall trends based on the space-time rainfall cube derived from 1981 to 2016
25 CHIRPS satellite rainfall data. The space time rainfall trend analysis revealed a significant (P
26 < 0.05) decrease of rainfall across most biomes particularly in the northern parts of the savanna
27 biome and southwestern biomes (i.e. karoo, desert and fynbos). Statistically significant ($P <$
28 0.05) rainfall increase was observed in the central parts of the region mostly within the savanna
29 biome. In terms of the magnitude of rainfall change, some of the areas experienced as much as
30 12 mm rainfall decrease in the mean annual rainfall while others recorded an increase of 14
31 mm. Our results provide baseline information for climate change adaptation and ecosystem
32 conservation.

33
34 **Key words:** Rainfall trend; Southern Africa; biome; climate change; drought

35

36
37

38

1 INTRODUCTION

39 The United Nations has identified global climate change as a key challenge of the 21st century
40 (Davis-Reddy and Vincent, 2017) with serious threats to ecosystems and society (Gosling et
41 al., 2011). Within southern Africa, severe and widespread droughts have occurred during
42 1982–1984, 1991–1992, and recently the 2015–2016 season drought was the driest since the
43 early 1980s with critical impacts on ecosystems and food security (Archer et al., 2017).
44 Furthermore, most parts in Africa are projected to have a possible decrease in rainfall as a result
45 of global warming (Mazvimavi, 2010).

46

47 The global warming effects together with expanding population and the resulting increased
48 pressure on ecosystems could lead to negative impacts on southern African societies which are
49 predominantly rural and survive on natural ecosystems (Dalal-Clayton, 1997). Studies claim
50 that global warming will result in extreme weather events (droughts and floods) (Fauchereau
51 et al., 2003). However, the magnitude of these extreme events is not known (Kusangaya et al.,
52 2013). This is despite the fact that these extreme events often have devastating consequences
53 on society for example the cyclone Idai which started on the 14th of March 2019 affected
54 Mozambique, Zimbabwe and Malawi killing more than 1000 people and destroying more than
55 50 000 houses (Reliefweb, 2019). The recent 2015/2016 drought season which caused severe
56 crop and ecosystem failure in the region (Archer et al., 2017) also points to the region's
57 vulnerability to the effects of global warming. It is therefore imperative to assess the historical
58 rainfall trends in order to understand future rainfall trends so that societies can be better
59 prepared especially in the case precipitation decreases.

60

61 The literature on historical rainfall trends in southern Africa is scanty and fragmented and based
62 on point level analysis (Kusangaya et al., 2013). The paucity of this literature was raised as a
63 major concern in the second assessment report of the Intergovernmental Panel on Climate
64 Change (IPCC) which noted insufficient studies on observed historical trends in climate
65 extremes (Toggweiler, 2001). Most of the available studies on rainfall trends are at country and
66 river basin level e.g. Kampata et al. (2008) found no evidence of significant trends in the annual
67 rainfall at individual stations of the Zambezi basin in Zambia. (Mazvimavi, 2010) also found

68 no evidence of significant trends in rainfall on all 40 weather stations used in Zimbabwe.
69 Fauchereau et al. (2003), did a similar study over southern Africa (1950-1988) and found no
70 significant changes in the late (January-March) season rainfall.

71
72 A comprehensive review of rainfall trend studies covering southern Africa was done by
73 Kusangaya et al. (2013). (Nicholson, 1993) analysed rainfall trends between the 1970-1990
74 period based on rain gauge data. The results of the study showed negative rainfall trends across
75 the whole African continent except for East Africa. A study by (Shongwe et al., 2009) revealed
76 decreasing rainfall trend in the southwestern parts of southern Africa and increasing rainfall
77 trend in the northern parts of the region mainly covering northernmost parts of Zambia, Malawi
78 and Mozambique. A similar study on rainfall trend analysis (1961-2000) based on ground
79 rainfall station data by (New et al., 2006) in Southern Africa also found negative rainfall trends
80 across most rainfall stations. On the contrary a study by (Joubert et al., 1996) revealed a
81 declining trend of rainfall for southern Africa. However, this decline was not statistically
82 significant. Statistically significant rainfall decrease in areas between the equator and 20° South
83 Latitude was reported by (Morishima and Akasaka, 2010) between 1979-2007 period.

84
85 The major weakness of these studies is that they do not simultaneously consider space and time
86 in the trend analysis and they are restricted to the location of rain gauges which are limited in
87 spatial coverage (Chikodzi and Mutowo, 2014). By considering time separately in rainfall trend
88 analysis, the existing studies fail to detect rainfall trend clusters which are slowly emerging
89 whilst considering space separately might detect less relevant rainfall trend clusters, i.e. those
90 that have been in existence over a long time, rather than emerging ones (Neill et al., 2005).
91 Furthermore, the analysis of rainfall trends at administrative or river basin level does not always
92 reflect southern Africa's main rainfall zones. In addition, such analysis cannot be extrapolated
93 to the southern African regional level mainly due to the use of different methodologies and
94 datasets check for reference.

95
96 Global circulation models provide an alternative source of regional information on rainfall
97 trends. However, the problem with these models, is that they do not accurately model regional
98 trends and different models sometimes show conflicting results of rainfall trends. For example,
99 (Dai, 2013) in a study entitled "Increasing drought under global warming in observations and

Commented [Moses@1]: How is our study different from Kusangaya.

Its preferable to cite a study and immediately raise the weaknesses.

Commented [Moses@2]: Check the referencing format and correct

Commented [Moses@3]: correct

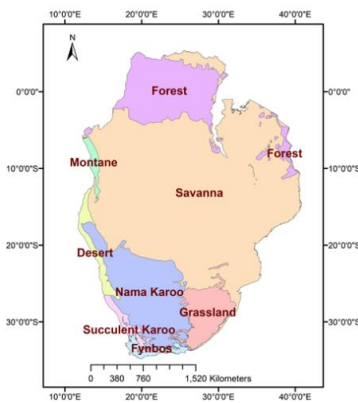
100 models” reported an increase of drought risk due to precipitation decreases over Africa. On the
101 other hand, (Trenberth et al., 2013) found no significant increase in drought trends. The
102 differences in the results of these two studies are partly attributed to different methodologies
103 used (Seneviratne, 2012).

104

105 In this regard, the aims of the study are to: (i) investigate the intra-annual and inter-annual
106 rainfall patterns over the southern African biomes, (ii) determine if there is any significant trend
107 in the long-term rainfall amounts over space and time and (iii) compute, on a pixel level the
108 magnitude of the rainfall change (total increase or decrease of rainfall (mm)) over a 36-year
109 period (1981-2016) across southern African biomes. We hypothesize the presence of negative
110 rainfall trends across southern African biomes due to increased frequency and intensity of
111 droughts.

112 2. METHODS

113 The study area, southern African biomes lies between latitude 6°N to 35°S and longitude 10°E
114 to 41°E (Figure 1). In terms of precipitation, the southern African rainy season is between
115 October and April for summer rainfall biomes i.e. desert, karoo, savanna and grassland, with
116 peak rainfall received between December and February. The fynbos biome receives winter
117 rainfall between May and September.



118

119 Figure 1: location of study area showing southern African biomes used in the rainfall trend analysis.

120

121 The El Niño Southern Oscillation (ENSO) controls inter-annual rainfall variability over the
122 Southern African. The ENSO phenomenon is triggered by variations in sea-surface temperature
123 (SST) in the equatorial Pacific (Unganai and Kogan, 1998). The El Niño (i.e. warm phase of
124 the ENSO) result in below average rainfall over greater parts of the region while the La Niña
125 (i.e. cold phase of ENSO) results in above average rainfall which normally leads to flooding.
126 Some of the strongest El Niño events are 1982/83 and 2015/16 rainfall seasons which resulted
127 in severe droughts (Davis-Reddy & Vincent, 2017). These two ENSO phases do not necessarily
128 occur in a sequence and have been reported to occur every three to seven years (OCHA, 2019).
129 In terms of duration, El Niño events rarely go beyond one year whilst La Niña events can go
130 up to three years (OCHA, 2019) reaching peak during the November to February for the
131 summer rainfall regions and March to June for the winter rainfall regions.

132

133 Greater part of the region's summer rainfall is also associated with latitudinal movement of the
134 Inter-Tropical Convergence Zone (ITCZ) and Congo air boundary (CAB) (Junginger and
135 Trauth, 2012). CAB is a belt of converging airstreams that create a belt of low pressure which
136 results in high rainfall (Marchant et al., 2007). During the summer, the ITCZ and CAB moves
137 southwards causing widespread rainfall especially when the ITCZ and CAB converge (Nash
138 and Endfield, 2002). The dry season occurs when the ITCZ and CAB moves northwards
139 (Unganai & Kogan, 1998).

140

141 Also important in regulating southern African rainfall is the Indian Ocean Dipole (IOD), which
142 refers to the difference in sea surface temperatures in the eastern and western part of the Indian
143 ocean (Marchant et al., 2007). The western Indian Ocean characterised by abnormally warm
144 (SSTs) whilst and the eastern Indian Ocean is characterised by abnormally cold SSTs
145 (Marchant et al., 2007). During the positive IOD warmer sea surface water moves towards the
146 western Indian ocean which increases rainfall over Africa and causes drought in Australia. The
147 negative IOD has an opposite effect, strong winds push warm water towards Australia which
148 result in less rainfall over Africa . (Marchant et al., 2007). Unganai and Kogan (1998) noted
149 that southern Africa's climate is also governed by the semi-permanent subtropical high-
150 pressure systems and by the downward leg of the Hadley cell which results in low rainfall. As
151 a result greater parts of southern African biomes are semi-arid (Unganai & Kogan, 1998) with
152 recurrent droughts.

2.1 Rainfall data

The study investigated the spatio-temporal rainfall trends over southern African biomes using Climate Hazards Group InfraRed Precipitation with Stations (CHIRPS) v2 satellite rainfall data covering the period 1981-2016. The CHIRPS rainfall data was generated by the U.S. Geological Survey Earth Resources Observation and Science Center in collaboration with the Santa Barbara Climate Hazards Group at the University of California (Funk et al., 2014). These data are available online at: <http://chg.geog.ucsb.edu/data/chirps/>. CHIRPS rainfall is developed by blending satellite based and climate models rainfall estimates, precipitation climatology and rainfall data from meteorological stations (Funk et al., 2014). The resultant data is provided at pentad, dekadal and monthly temporal resolution on a 0.05° spatial resolution and is available from 1981 to present. The main advantages of the CHIRPS satellite rainfall data is that it incorporates more meteorological station rainfall data than other satellite rainfall estimates products which help to improve its accuracy (Shukla et al., 2014). The CHIRPS data set has been shown to correlate with other global data sets such as the Global Precipitation Climatology Project (GPCP) (Shukla et al., 2014).

We analysed the rainfall trends at biome level (Figure 1). Biomes generally follow the main climatic regions (Mucina and Rutherford, 2006) which makes them ideal for rainfall trend analysis. The biome data used in the study is based on the Terrestrial Ecoregions of the World data developed by (Olson et al., 2001). These data can be downloaded freely from the WWF website (<https://www.worldwildlife.org/publications/terrestrial-ecoregions-of-the-world>).

2.2 Rainfall trend analysis

In this study, we analysed the seasonal annual rainfall trends using October to April for the summer rainfall biomes and May to September for the Fynbos biome which receive rainfall in winter. For October to April annual season, we divided the rainfall season into two main parts as follows; (a) the early part of the rainy season, October-November-December (OND), and (b) the mid to end of the rainfall season, January-February-March (JFM). The rationale behind splitting the season into two parts is that most parts of the vegetated landscape of southern Africa are predominantly deciduous with vegetation greening up during the October to December period (Chidumayo, 2001; Cho et al., 2017). Thus the variations of OND rainfall will have an impact on the early stages of vegetation development, while the JFM rainfall

185 variations will impact the final phases of vegetation development (Mazvimavi, 2010). The
186 division of the rainfall into two parts also help to capture trends that may not be identified in
187 the total annual precipitation

188

189 **2.2.1 Intra-annual and Inter-annual patterns**

190 In the context of rainfall trend analysis, intra-annual refers to rainfall variation that occur at a
191 time scale of 1 year and inter-annual refers to rainfall variation across the years. In order to
192 understand intra-annual historical rainfall trends, we computed the rainfall z-score
193 (standardised difference) from 10 days and seasonal rainfall data. The z-score defines the
194 number of standard deviation (anomaly) from the average i.e. decadal or seasonal long-term
195 average (1981-2016). Z-score values can either be positive or negative, indicating whether the
196 parameter i.e. rainfall is above or below the decadal or seasonal long-term average and by how
197 many standard deviations. Standard deviation within the range of 1 to -1 is considered to be
198 within the normal range. We computed the rainfall z-score for each biome using the following
199 (Eq. 1)

$$200 \quad Z_{ij} = \frac{x_{ij} - \bar{x}_i}{\sigma_i} \quad (\text{Eq.1})$$

201 Where Z_{ij} is the z-score; x_{ij} is the raw input value to be standardised; \bar{x}_i is the mean of the
202 population and σ_i is the standard deviation.

203

204 **2.2.2 Spatio-temporal trends**

205 To test the hypothesis of the presence of negative rainfall trends, we used a space-time cube
206 approach which enables the detection of statistical hot (wet spells i.e. high rainfall clusters) and
207 cold spots (dry spells i.e. low rainfall clusters) (Gates, 2017). A space time cube is a 3
208 dimensional data structure which is based on geographic coordinates (x and y) and z coordinate
209 representing time (Abdrakhmanov et al., 2017). The space-time cube approach is important in
210 rainfall trend analysis and it was successfully used to analyse the anthrax epidemic among
211 livestock in Kazakhstan over the period 1933-2016 (Abdrakhmanov et al., 2017). The same
212 approach can be applied to spatio-temporal rainfall analysis. Analysing rainfall data over space
213 and time can show previously unknown trends (Gates, 2017) and provide answers to questions
214 such as: where are the space-time drought hot spots located? ; are these hot-spot patterns /
215 trends new, intensifying, persistent, or sporadic hot-spot patterns? (ESRI, 2018).

216 We analysed the rainfall space-time trends based on a space-time rainfall cube covering 125 x
217 125km using the emerging hotspot tool in ArcGIS software (ESRI, 2018). Each cube (bin)
218 represents the rainfall station location, time and the rainfall value. The rainfall space-time cube
219 approach enables the detection of rainfall trend clusters through time and shows areas or
220 clusters with increasing or decreasing rainfall We selected this tool because of ability to
221 simultaneously handle space and time in trend analysis. This tool takes as input a space-time
222 Network Common Data Form (NetCDF) cube and then identifies trends in data using Mann-
223 Kendall trend test (ESRI, 2016). The resulting trends from the emerging hotspot tool are
224 classified either as new, intensifying, diminishing, and sporadic hot and cold spots (Figure 4)
225 (ESRI, 2018). The Mann-kendall trend test, is a nonparametric test which is used for detecting
226 trends in time series data and is extensively used in rainfall and river discharge time series data
227 (Kendall, 1945). The Mann-kendall trend test correlation coefficient, tau which ranges from -
228 1 and 1 provides the direction and strength of the trend in a time series. The advantages of the
229 Mann-Kendall test over the Spear-man's rho test is that it less affected by small numbers of
230 extreme outliers and it can also work with missing data (Croux and Dehon, 2010).

231
232 We first calculated the intensity of clustering for both high and low rainfall values based on the
233 Getis-Ord G_i^* statistic for each rainfall cube representing location of a weather station. The
234 Getis-Ord G_i^* statistic, introduced by Getis and Ord provides an indication of where
235 observations with either low or high values cluster. Locations of high spatial associations /
236 clustering will have positive z-score (Songchitruksa and Zeng, 2010). On the other hand,
237 negative z-score provides an indication of clustering of low values .We then evaluated the
238 trends for the dry and wet spells using the Mann-Kendall trend test to detect whether a
239 decreasing or increasing trend is present in the rainfall space time cube (Kendall, 1945; Gates,
240 2017). The resultant map of the rainfall trends with the associated z-score and p values is shown
241 in Figure 5.

242
243 **2.2.3 Quantification of the magnitude of the trend (rainfall increase or decrease)**
244 We first computed pixel-wise Mann-Kendall tau correlation coefficient to establish the
245 direction of the rainfall trends. To quantify the magnitude of the trend i.e. total decrease or
246 increase of rainfall (mm) over time, we computed a pixel-wise linear regression using time
247 (years) as independent and annual rainfall as dependent variables. Here, the slope of the
248 regression which gives the increase or decrease of rainfall was computed using a linear model

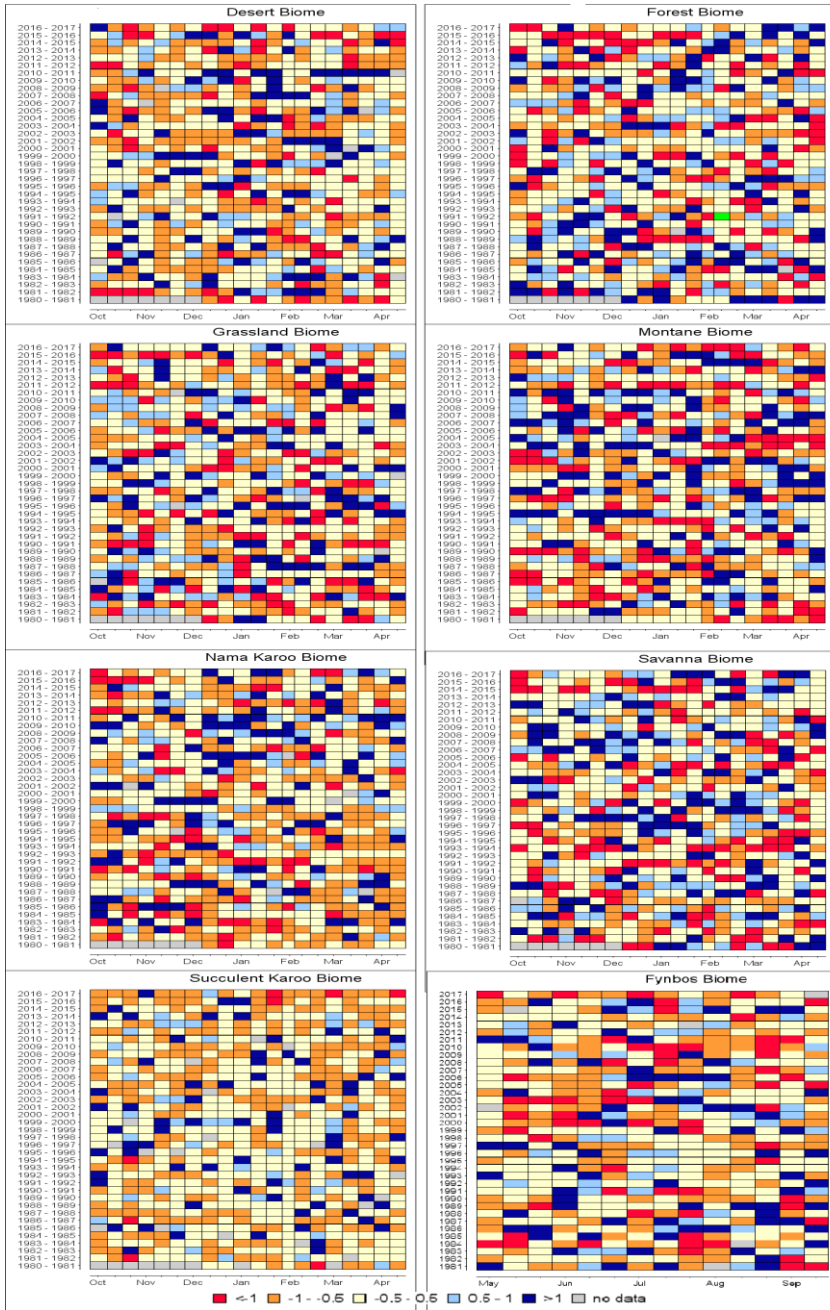
249 and raster package within the statistical software environment (R Core Team, 2018). The
250 resultant average slope map was multiplied by the number of years (1981-2016) i.e. 36 years
251 to determine the magnitude of the trend.

252 **3 RESULTS AND DISCUSSIONS**

253 **3.1 Intra-annual and inter-annual rainfall trends**

254 Figure 2 displays the intra-annual variability based on 10-day rainfall z-scores for the 36-year
255 period (1981-2016) aggregated over the biomes. Negative Z-scores, representing below normal
256 rainfall were mostly recorded in recent years, between 2014-2016 seasons mostly in the arid
257 and semi-arid biomes. These negative z-score (i.e. dry spell) mainly occur between the October
258 to December period for most biomes except the montane biome (Figure2).

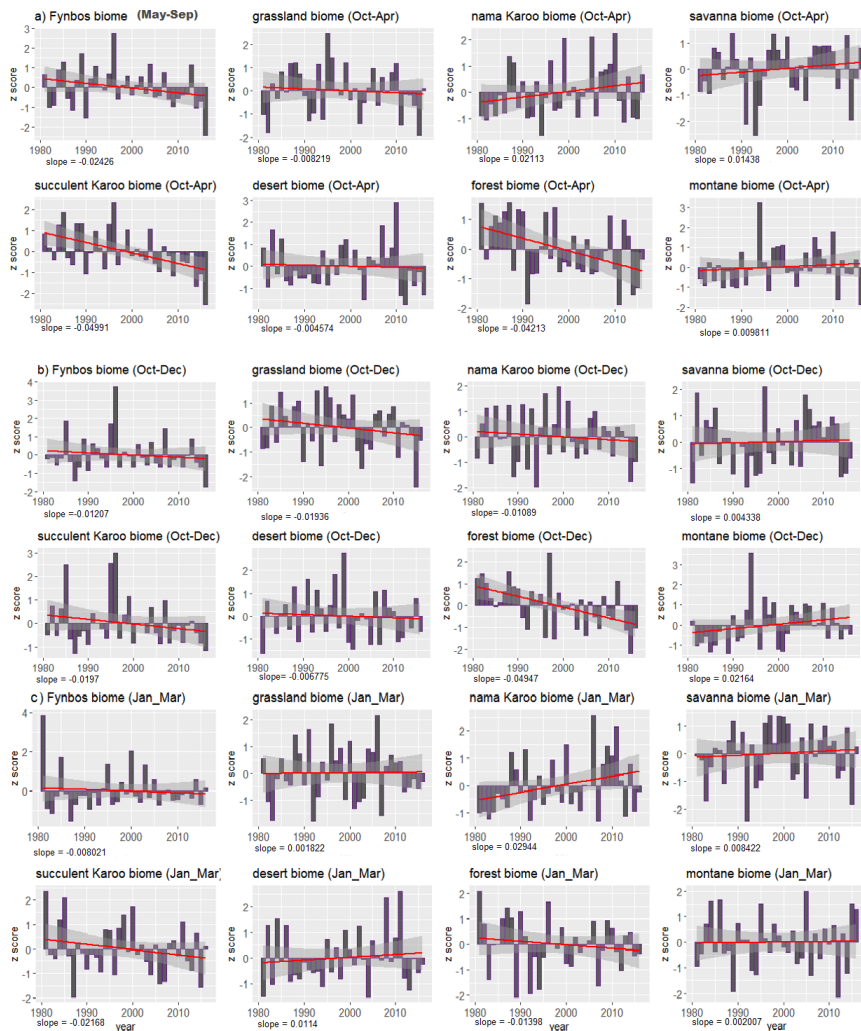
259



260

261 Figure 2: Intra-annual rainfall trends based on 10-day rainfall z-scores.

262 A summary of the inter-annual rainfall trends is presented in Figure 3. At the seasonal annual
263 time scale and during the October to December period (Figure 3a and b), we observe negative
264 rainfall trend in all biomes except for the savanna, nama karoo and montane biomes which
265 show an increasing rainfall trend. More biomes (grassland, desert, nama karoo, savanna and
266 montane) show an increasing rainfall trend during the January to March period (Figure 3c).
267 This might be attributed to the fact that this is the period when most cyclones in Southern Africa
268 to occur. At the annual time scale, the succulent karoo biome has the steepest decrease of
269 rainfall (slope= -0.04991) (Figure 3a). This is followed by the forest biome (slope = -0.04947)
270 (Figure 3b). The observed increasing rainfall trend at the annual time-scale in the nama karoo
271 biome (Figure 3a) is not statistically significant for greater part of the biome (Figure 6b)



272

273 Figure 3: *Inter-annual trends for: (a) annual rainfall (October-April for summer rainfall*
 274 *biomes and May-September for winter rainfall biomes); (b) early rainfall season (October-*
 275 *December) and (c) mid to late rainfall season (January-March)*

276 3.2 Spatio-temporal analysis

277 The analysis of the rainfall space-time cube showed a decreasing rainfall trend (dry spells, blue
 278 colour (Figure 4) across all the arid biomes, which are located in the south and southwestern
 279 parts of the region covering mostly the karoo, desert, fynbos biomes and western parts of the
 280 grassland biome. The decreasing trend is also observed in the forest biome during the late part

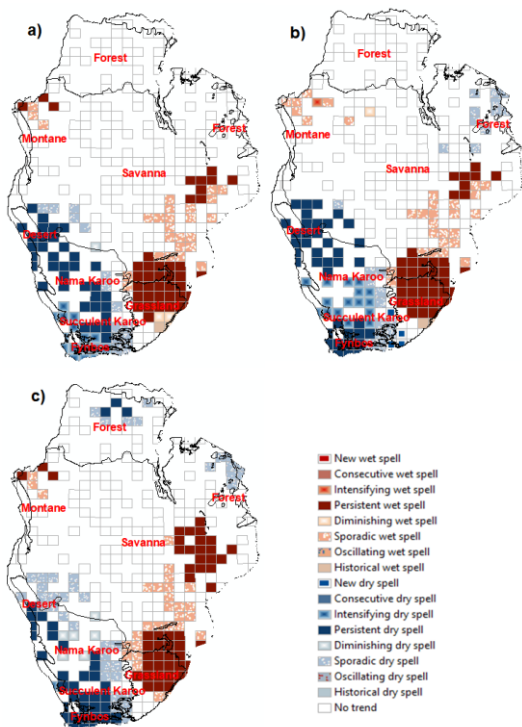
281 of the season (i.e. January to March period). Cluster of increasing rainfall trends (wet spells,
 282 brown colour) are mainly found in the montane, grassland and western and central parts of the
 283 savanna region. We did not observe significant trend in the space time rainfall cube over greater
 284 parts of the savanna and the forest biome (Figure 4a)

285

286 We observed the intensification of the dry spells (clusters of low rain) over the fynbos and
 287 karoo biomes (Figure 4). This area has been noted by the South African National Biodiversity
 288 Institute (SANBI) as an area of high concentrations of taxa of conservation concern (SANBI,
 289 2017). The other concern is the persistent dry spells mainly over the forest biome during the
 290 January to March period (Figure 4c, blue colour).

291

292



293

294 *Figure 4: Space-time rainfall trend based on 125X125km grid for: (a) annual rainfall (October-April for summer*
 295 *rainfall biomes and May-September for winter rainfall biomes); (b) early rainfall season (October-December)*
 296 *and (c) mid to late rainfall season (January-March).*

297

298 Table 1: Regional summary of space-time rainfall trends.

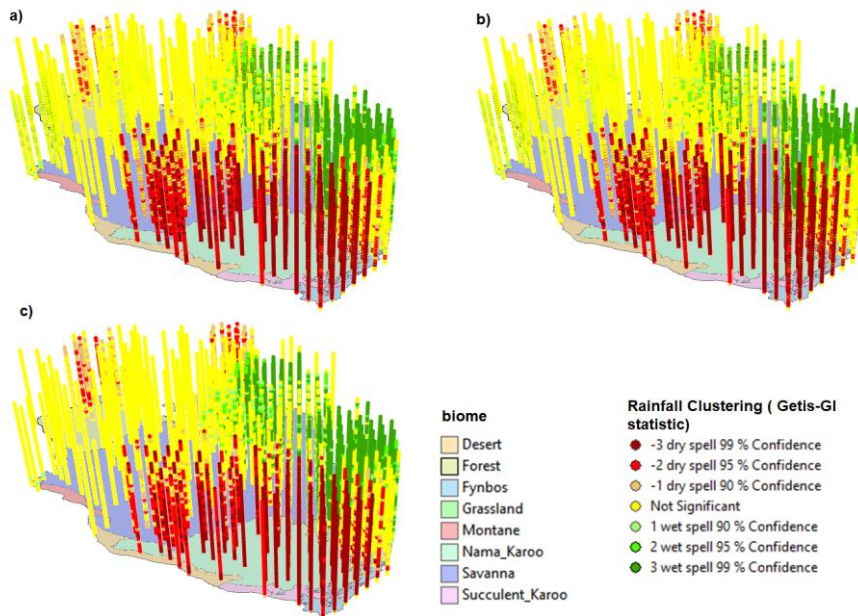
	Wet spell	dry spell		Wet spell	dry spell		Wet spell	dry spell
New	0	0	New	0	5	New	0	0
Consecutive	0	0	Consecutive	0	0	Consecutive	0	0
Intensifying	0	17	Intensifying	1	16	Intensifying	0	2
Persistent	41	36	Persistent	33	39	Persistent	48	38
Diminishing	4	1	Diminishing	1	0	Diminishing	0	6
Sporadic	26	16	Sporadic	12	26	Sporadic	10	39
Oscillating	0	0	Oscillating	0	0	Oscillating	0	0
Historical	1	0	Historical	1	0	Historical	0	0
Seasonal annual rainfall			October to December season rainfall			January to March season rainfall		

299

300 Table 1 show the summary of the space-time rainfall trends for all biomes. What is of more
 301 concern is the intensification of the dry spells for all the three periods. This trend has negative
 302 consequences on the vegetation development especially for the south western biomes.

303 To get an insight into the evolution of space-time rainfall trends shown in Figure 4, we
 304 developed a 3-dimensional map of the space-time rainfall cube (Figure 5). For the first time,
 305 we were able to simultaneously observe the spatio-temporal trends of wet and dry spell clusters
 306 over southern African biomes. We observed intense clustering of dry spells over the desert and
 307 karoo biomes (Figure 5).

308



309

310 Figure 5: 3-dimensional visualisation of the rainfall space-time cube hot spot

311

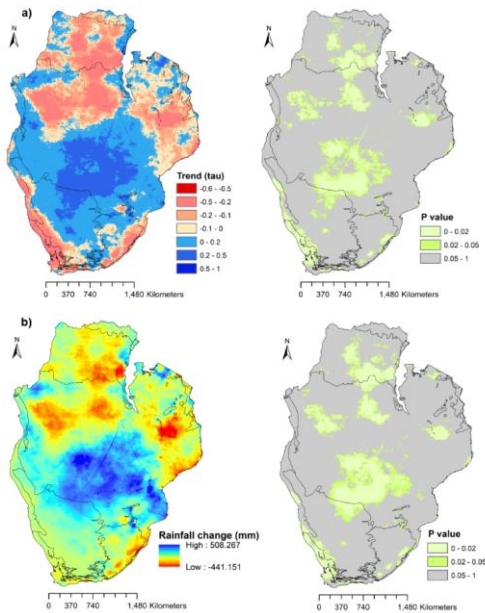
312 3.3 Magnitude of Rainfall change (mm)

313 Results of the pixel-wise Mann-kendall trend analysis are presented in Figure 6a. Statistically
314 significant ($p < 0.05$) negative rainfall trend was mainly observed over the desert, succulent
315 karoo, fynbos, northern part of the savanna and western parts of the grassland biome (Figure
316 6a). We observed statistically significant increasing rainfall mainly over the central part of the
317 southern African region covering the savanna biome. We did not observe any statistically
318 significant trend for the montane biome (Figure 6a).

319

320

321



322
 323 Figure 6: a) Annual rainfall trend based on Mann-Kendall tau and associated p values b) the magnitude of
 324 annual rainfall change i.e. rainfall increase (+) or decrease (-) in mm and associated p values

325
 326 The results from the pixel-wise linear regression showed a decrease in annual rainfall up to 441
 327 mm and an increase up to 508mm between 1981 and 2016 (Figure 6b). The highest statistically
 328 significant decrease is observed over the northern parts of the southern African region
 329 bordering the savanna and forest biome (Figure 6b). The highest increase in rainfall change
 330 (over a 36-year period) observed over the central parts of the region might be explained by the
 331 fact that this is area which is mostly affected by the tropical cyclones which have been on the
 332 increase in recent years.

333 4. DISCUSSION AND CONCLUSION

334 Historical rainfall trend information is important in many areas such as health, farming,
 335 ecosystems, hydrology, etc. We analysed CHIRPS satellite rainfall data to determine rainfall
 336 trends over a 36-year period for eight southern African biomes. The results of the Mann-
 337 Kendall trend analysis revealed a negative rainfall trend mainly over the forest biome and
 338 southern western parts of the region (i.e. fynbos, desert and karoo biomes). Increasing rainfall

339 trend was mainly observed in the central parts of the region and western parts of the savanna
340 biome. Our results are in line with the findings of (Shongwe et al., 2009) who observed
341 declining rainfall trends over the southwestern parts of the Southern African region and
342 increasing trends in northern part of Mozambique, Zambia and Malawi

343

344 Most of the areas with negative rainfall trends have been reported by (Sloat et al., 2018) to have
345 a high coefficient of variation of rainfall (CVP) (unreliable rainfall patterns). The rainfall
346 decline is largely attributed to the effects of warm phases of the El Niño-Southern Oscillation
347 (ENSO) which result in drought conditions over southern Africa (Gaughan and Waylen, 2012).
348 In recent years (2014-2017), El Niño events have been on the increase with the 2015-2016 El
349 Niño being the strongest since the 1970s (weathertrends360, 2015). This explains the declining
350 rainfall trends across the southern African biomes. It is also important to note that areas with
351 increasing rainfall trend mostly over the Nama karoo biome are not statistically significant at
352 5% significance level. One possible explanation might be the reliability of rainfall as reported
353 by (Sloat et al., 2018).

354

355 The declining rainfall trends will have negative impacts on the southern African population
356 due to the low adaptive capacity (Kusangaya et al., 2013). For example, within the fynbos
357 biome, the decline in rainfall activity has already led to water restrictions by the Cape town
358 municipality in South Africa following the 2015-2017 drought (Western Cape Government,
359 2019). The declining rainfall in the southern parts of the grassland biome which mainly covers
360 greater parts of South Africa has a negative impact on livestock production. Within the
361 grassland biome, livestock grazing is key for local communities as well as the beef industry.
362 Sloat et al. (2018) in a study entitled "Increasing importance of precipitation variability on
363 global livestock grazing lands" assessed the inter- and intra-annual precipitation-based threats
364 to global rangelands based on rainfall concentration index, NDVI, coefficient of variation of
365 rainfall (CVR) and livestock density data. The major finding of the study was that areas with
366 unreliable rainfall, i.e. high CVR such as the grassland and savanna biome have low carrying
367 capacity than less variable regions. The study further reports globally the rangelands have a
368 CVR of 0.27, which is 25 percent more than all land surfaces combined (Patel, 2019). This
369 high CVR coupled with the declining rainfall trends reported in this study affects the livestock
370 carrying capacity (Patel, 2019).

371

372 For management purpose, since most of the severe rainfall decreases have been observed in
373 the northern savanna and western parts of grassland biomes and also considering the fact that
374 these biomes are mostly used for grazing compared to any other activity (Patel, 2019),
375 destocking is recommended. In addition (Sloat et al., 2018) recommends the efficient use of
376 the biomes grazing landscape as well as the avoidance of cultivation in these marginal
377 landscapes. Results from this study provides baseline data for climate change mitigation
378 programmes as well as mapping drought hotspots. Future studies should focus on trend analysis
379 based on day-count indices e.g. number of days with rainfall amount higher than 1mm as
380 recommended by World Meteorological Organisation.

381

382 **5 FUNDING**

383 This work was supported by the University of Pretoria Postgraduate Doctoral Bursary.

384 **6 AUTHORS CONTRIBUTION**

385 Study conception and design: Marumbwa, Cho
386 Acquisition of data: Marumbwa
387 Analysis and interpretation of data: Marumbwa, Cho
388 Drafting of manuscript: Marumbwa
389 Supervision: Cho and Chirwa
390 Critical revision: Cho, Marumbwa

391

392 **Conflicts of Interest:** The authors declare no conflict of interest.

393 **7 ACKNOWLEDGMENTS:**

394 We thank Thembani Moithobogi for his assistance in the development of some data processing
395 scripts

396

397 **8 REFERENCES**

398 Abdrakhmanov SK, Mukhanbetkaliyev YY, Korennoy FI, et al. (2017) Spatio-temporal
399 analysis and visualisation of the anthrax epidemic situation in livestock in Kazakhstan
400 over the period 1933-2016. *Geospatial Health* 12: 316-324.

401 Archer ERM, Landman WA, Tadross MA, et al. (2017) Understanding the evolution of the
402 2014–2016 summer rainfall seasons in southern Africa: Key lessons. *Climate Risk*
403 *Management* 16: 22-28.

404 Chidumayo EN. (2001) Climate and Phenology of Savanna Vegetation in Southern Africa.
405 *Journal of Vegetation Science* 12: 347-354.

406 Chikodzi D and Mutowo G. (2014) Remote sensing based drought monitoring in Zimbabwe.
407 *Disaster Prevention and Management: An International Journal* 23: 649-659.

408 Cho MA, Ramoelo A and Dziba L. (2017) Response of Land Surface Phenology to Variation
409 in Tree Cover during Green-Up and Senescence Periods in the Semi-Arid Savanna of
410 Southern Africa. *Remote Sensing* 9.

411 Croux C and Dehon C. (2010) Influence functions of the Spearman and Kendall correlation
412 measures. *Statistical Methods & Applications* 19: 497-515.

413 Dai A. (2013) Increasing drought under global warming in observations and models. *Nature*
414 *Climate Change* 3: 52.

415 Dalal-Clayton B. (1997) *SOUTHERN AFRICA BEYOND THE MILLENIUM: ENVIRONMENTAL TRENDS AND SCENARIOS TO 2015*. , London. GB. 1997.
416 International Institute for Environment and Development. Impreso. 104 p.. :
417 Environmental monitoring.

419 Davis-Reddy CL and Vincent K. (2017) *Climate Risk and Vulnerability: A Handbook for*
420 *Southern Africa* (2nd Ed). CSIR, Pretoria, South Africa.

421 ESRI. (2016) *How Emerging Hot Spot Analysis works*. Retrieved 16 January 2017. Available
422 at: [http://desktop.arcgis.com/en/arcmap/10.3/tools/space-time-pattern-mining-
423 toolbox/learnmoreemerging.htm](http://desktop.arcgis.com/en/arcmap/10.3/tools/space-time-pattern-mining-toolbox/learnmoreemerging.htm).

424 ESRI. (2018) *Emerging Hot Spot Analysis*. Retrieved 18 January 2018. Available at:
425 [http://pro.arcgis.com/en/pro-app/tool-reference/space-time-pattern-
426 mining/emerginghotspots.htm](http://pro.arcgis.com/en/pro-app/tool-reference/space-time-pattern-mining/emerginghotspots.htm).

427 Fauchereau N, Trzaska S, Rouault M, et al. (2003) Rainfall Variability and Changes in
428 Southern Africa during the 20th Century in the Global Warming Context. *Natural*
429 *Hazards* 29: 139-154.

430 Funk CC, Peterson PJ, Landsfeld MF, et al. (2014) A quasi-global precipitation time series for
431 drought monitoring. *Data Series*. Reston, VA, 12.

432 Gates S. (2017) *Emerging Hot Spot Analysis: Finding Patterns over Space and Time*. Retrieved
433 17 January 2018. Available at: [https://www.azavea.com/blog/2017/08/15/emerging-
434 hot-spot-spatial-statistics/](https://www.azavea.com/blog/2017/08/15/emerging-hot-spot-spatial-statistics/).

435 Gaughan AE and Waylen PR. (2012) Spatial and temporal precipitation variability in the
436 Okavango–Kwando–Zambezi catchment, southern Africa. *Journal of Arid*
437 *Environments* 82: 19-30.

438 Gosling SN, Warren R, Arnell NW, et al. (2011) A review of recent developments in climate
439 change science. Part II: The global-scale impacts of climate change. *Progress in*
440 *Physical Geography: Earth and Environment* 35: 443-464.

441 Joubert AM, Mason SJ and Galpin JS. (1996) DROUGHTS OVER SOUTHERN AFRICA IN
442 A DOUBLED-CO2 CLIMATE. *International Journal of Climatology* 16: 1149-1156.

443 Junginger A and Trauth M. (2012) *The Role of the Congo Air Boundary and Solar Variations*
444 *during the Early Holocene East African Humid Period.*

445 Kendall MG. (1945) *Rank Correlation Methods. 4th Edition.* , Charles Griffin, London.

446 Kusangaya S, Warburton ML, Archer van Garderen E, et al. (2013) Impacts of climate change
447 on water resources in southern Africa: A review. *Physics and Chemistry of the Earth,*
448 *Parts A/B/C 67-69: 47-54.*

449 Marchant R, Mumbi C, Behera S, et al. (2007) The Indian Ocean dipole – the unsung driver of
450 climatic variability in East Africa. *African Journal of Ecology* 45: 4-16.

451 Mazvimavi D. (2010) Investigating changes over time of annual rainfall in Zimbabwe. *Hydrol.*
452 *Earth Syst. Sci.* 14: 2671-2679.

453 Morishima W and Akasaka I. (2010) Seasonal Trends of Rainfall and Surface Temperature
454 over Southern Africa. *African study monographs. Supplementary issue.* 40: 67-76.

455 Mucina L and Rutherford M. (2006) *The vegetation of South Africa, Lesotho and Swaziland,*
456 *in Strelitzia 19.* South African National Biodiversity Institute, Pretoria.

457 Nash DJ and Endfield GH. (2002) A 19th century climate chronology for the Kalahari region
458 of central southern Africa derived from missionary correspondence. *International*
459 *Journal of Climatology* 22: 821-841.

460 Neill DB, Moore AW, Sabhnani M, et al. (2005) Detection of emerging space-time clusters.
461 *Proceedings of the eleventh ACM SIGKDD international conference on Knowledge*
462 *discovery in data mining.* Chicago, Illinois, USA: ACM, 218-227.

463 New M, Hewitson B, Stephenson DB, et al. (2006) Evidence of trends in daily climate extremes
464 over southern and west Africa. *Journal of Geophysical Research: Atmospheres* 111.

465 Nicholson SE. (1993) An Overview of African Rainfall Fluctuations of the Last Decade.
466 *Journal of Climate* 6: 1463-1466.

467 OCHA. (2019) *El Niño and La Niña.* Retrieved 8 April 2019. Available at:
468 <https://www.unocha.org/es/themes/el-niño/el-niño-and-la-niña>.

469 Olson DM, Dinerstein E, Wikramanayake ED, et al. (2001) Terrestrial Ecoregions of the
470 World: A New Map of Life on Earth: A new global map of terrestrial ecoregions
471 provides an innovative tool for conserving biodiversity. *BioScience* 51: 933-938.

472 Patel K. (2019) *Unstable Precipitation Leads to Unstable Pastures.* Retrieved 1 March 2019.
473 Available at: [https://earthobservatory.nasa.gov/images/144568/unstable-precipitation-](https://earthobservatory.nasa.gov/images/144568/unstable-precipitation-leads-to-unstable-pastures)
474 [leads-to-unstable-pastures.](https://earthobservatory.nasa.gov/images/144568/unstable-precipitation-leads-to-unstable-pastures)

475 R Core Team. (2018) R: A language and environment for statistical computing. R Foundation
476 for Statistical Computing. Vienna, Austria.

477 SANBI. (2017) *Threatened Species Programme.* Retrieved 17 April 2018. Available at:
478 <http://redlist.sanbi.org>.

479 Seneviratne SI. (2012) Historical drought trends revisited. *Nature* 491: 338.

480 Shongwe ME, van Oldenborgh GJ, van den Hurk BJM, et al. (2009) Projected Changes in
481 Mean and Extreme Precipitation in Africa under Global Warming. Part I: Southern
482 Africa. *Journal of Climate* 22: 3819-3837.

483 Shukla S, McNally A, Husak G, et al. (2014) A seasonal agricultural drought forecast system
484 for food-insecure regions of East Africa. *Hydrol. Earth Syst. Sci.* 18: 3907-3921.

485 Sloat LL, Gerber JS, Samberg LH, et al. (2018) Increasing importance of precipitation
486 variability on global livestock grazing lands. *Nature Climate Change* 8: 214-218.

487 Songchitruksa P and Zeng X. (2010) *Getis–Ord Spatial Statistics to Identify Hot Spots by Using*
488 *Incident Management Data*.

489 Toggweiler JR. (2001) *Thermohaline Circulation*: Encyclopedia of Ocean Sciences.

490 Trenberth KE, Dai A, van der Schrier G, et al. (2013) Global warming and changes in drought.
491 *Nature Climate Change* 4: 17.

492 Unganai LS and Kogan FN. (1998) Drought Monitoring and Corn Yield Estimation in Southern
493 Africa from AVHRR Data. *Remote Sensing of Environment* 63: 219-232.

494 weathertrends360. (2015) *Strongest El Niño in 100 years! Here are some predictions.*
495 *Retrieved 27 May 2017. Available at:*
496 [http://www.weathertrends360.com/Blog/Post/Strongest-El-Nio-in-100-years-Here-](http://www.weathertrends360.com/Blog/Post/Strongest-El-Nio-in-100-years-Here-are-some-predictions-2506)
497 [are-some-predictions-2506.](http://www.weathertrends360.com/Blog/Post/Strongest-El-Nio-in-100-years-Here-are-some-predictions-2506)

498 Western Cape Government. (2019) *Cape Town water rationing. Retrieved 11 April 2019.*
499 Available at: [https://www.westerncape.gov.za/general-publication/cape-town-water-](https://www.westerncape.gov.za/general-publication/cape-town-water-rationing)
500 [rationing.](https://www.westerncape.gov.za/general-publication/cape-town-water-rationing)

501